A Study on the Curing Kinetics of Epoxycyclohexyl Polyhedral Oligomeric Silsesquioxanes and Hydrogenated Carboxylated Nitrile Rubber by Dynamic Differential Scanning Calorimetry

Qing Liu, Wentan Ren, Yong Zhang, Yinxi Zhang

State Key Laboratory of Metal Matrix Composites, School of Chemistry and Chemical Engineering, Shanghai Jiao Tong University, Shanghai 200240, China

Received 21 February 2010; accepted 23 May 2011
DOI 10.1002/app.34954
Published online 2 September 2011 in Wiley Online Library (wileyonlinelibrary.com).

ABSTRACT: A new organic–inorganic hybrid material was prepared through reactive blending of hydrogenated carboxylated nitrile rubber (HXNBR) with epoxycyclohexyl polyhedral oligomeric silsesquioxanes (epoxycyclohexyl POSS). The structure of the composite was characterized by Fourier transform infrared spectroscopy (FTIR) and solid-state ^{13}C Nuclear Magnetic Resonance spectra (solid-state ^{13}C-NMR). The differential scanning calorimetry (DSC) at different heating rates was conducted to investigate the curing kinetics. A single overall curing process by an nth-order function $(1 - \alpha)^n$ was considered, and multiple-heating-rate models (Kissinger, Flynn–Wall–Ozawa, and Crane methods) and the single-heating-rate model were employed. The apparent activation energy (E_a) obtained showed dependence on the POSS content and the heating rate (β). The overall reaction order n was practically constant and close to 1. The isoconversion Flynn–Wall–Ozawa method was also performed and fit well in the study. With the single-heating-rate model, the average E_a for the compound with a certain POSS content, 66.90–104.13 kJ/mol was greater than that obtained with Kissinger and Flynn–Wall–Ozawa methods. Furthermore, the calculated reaction rate ($d\alpha/dt$) versus temperature curves fit with the experimental data. © 2011 Wiley Periodicals, Inc. J Appl Polym Sci 123: 3128–3136, 2012

Key words: hydrogenated carboxylated nitrile rubber; epoxycyclohexyl POSS; curing kinetics; dynamic DSC

INTRODUCTION

Polyhedral oligomeric silsesquioxanes (POSS) have attracted great attention recently when various POSS-based nanocomposites have shown very improved properties. The POSS[1,2] molecule contains a cubic cage-like inorganic backbone consisting of Si and O, which can provide composites with enhanced mechanical properties, thermal stability, and oxidation resistance. POSS cages with various side groups have been incorporated into polymer matrices by blending or chemical bonding, forming novel thermoplastics or thermosets, such as epoxy,[3–6] amine,[7] vinyl,[8,9] and the like. Most of those studies focus on mechanical properties and morphologies of the composites.[2,3,5–13] Only a few of them try to investigate the kinetics[14,15] of the reaction. However, the curing kinetics will describe the curing cycle used in processing, which is fundamentally important for determining the property of the materials.

Hydrogenated carboxylated nitrile rubber (HXNBR) is a high performance rubber with excellent mechanical properties, abrasion resistance, thermal stability, and oxidation resistance. It is used in many applications.[16] However, it has relatively poor dielectric and hydrophobic properties due to carboxyl and cyano groups. Incorporation of epoxy POSS into HXNBR by chemical bonding will form a new crosslinked hybrid material with a lowered dielectric constant and an improved hydrophobic property. Therefore, it is fundamental for us to study the curing kinetics for the new organic–inorganic hybrid material, which will describe the curing cycle to be used in processing.

Many different analytical methods have been employed to study the curing kinetics by some earlier reports, such as differential scanning calorimetry (DSC),[14,15] Fourier transform infrared (FTIR),[17,18] chemorheological study,[19] vibrational spectroscopy,[20] nuclear magnetic resonance (NMR), and gel permeation chromatography (GPC).[21] Considering their difference in the sample preparation requirement, the temperature-scanning precision, and the signal-recording continuity, we employed DSC to study the curing kinetics for epoxycyclohexyl POSS/HXNBR.

Correspondence to: W. Ren (1958rwt@sjtu.edu.cn).
Contract grant sponsor: National Natural Science Foundation of China; contract grant numbers: 50773036, 51073092.

In this work, a new organic–inorganic hybrid material is prepared through reactive blend of HXNBR with epoxycyclohexyl POSS. The curing kinetics is studied by the multiple-heating-rate models (the Kissinger, Flynn–Wall–Ozawa, and Crane methods) and the single-heating-rate model, and the reaction rate ($d\alpha/dt$) versus temperature curve according to the calculated kinetic parameters is compared with the experimental data.

EXPERIMENTAL

Materials

HXNBR (Therban XT VP KA 8889) containing 33% acrylonitrile, 5% carboxylic acid, and 3.5% residual double bonds was produced by LANXESS Deutschland GmbH and its Mooney viscosity ML (1 + 4) at 100°C is 77. Epoxycyclohexyl POSS (EP0408, liquid at room temperature) was purchased from Hybridplastic (Hattiesburg, USA) and used as received. Chemical structure representation of epoxycyclohexyl POSS $((C_8H_{13}O)_m(SiO_{1.5})_m$, $m = 8, 10, 12)$ is shown in Figure 1.

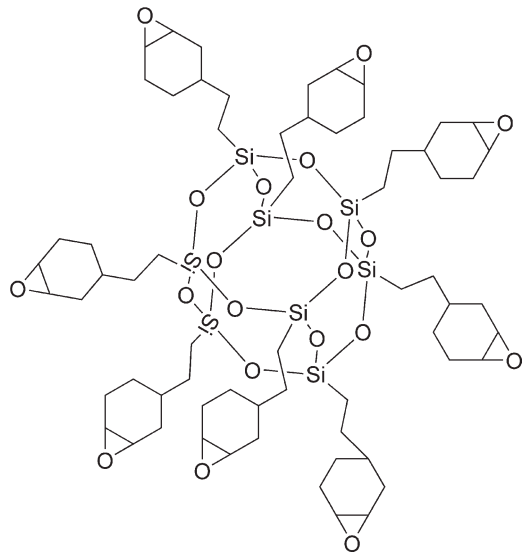

Figure 1 Chemical structure representation of epoxycyclohexyl POSS ($m = 8$ shown).

Sample preparation

Epoxycyclohexyl POSS/HXNBR compounds were prepared through a two-stage mixing procedure. HXNBR solutions in tetrahydrofuran (THF, boiling point 66°C) containing 0, 2, 5, 10, and 40 phr (per hundred rubber by weight) epoxycyclohexyl POSS were stirred for 4–6 h and cast onto Teflon slot dies. The solvent was left to evaporate at room temperature for 36 h. The obtained compound film was vacuum dried at room temperature for 24 h to remove the residual solvent. The compounds were then processed with a two-roll mill at room temperature to get a good blending. The composites were prepared by curing the compounds at 190°C for 20 min under pressure of 10 MPa.

Characterization techniques

Equilibrium swelling method was used to determine the crosslink density of the composites. The samples were first weighed for initial dry weights and then swollen in THF at room temperature. Periodically, swollen weights of the samples were measured until equilibrium weights were obtained. The samples were then vacuum dried for 36 h at 80°C and reweighed for the final dry weights. The volume fraction ($_r$) of the rubber in the composites which were swollen to equilibrium was calculated by the following equation[22] to represent the crosslink density,

$$\upsilon_r = \frac{m_0\phi(1-\alpha)/\rho_r}{m_0\phi(1-\alpha)/\rho_r + (m_1 - m_2)/\rho_s} \quad (1)$$

where m_0 is the sample mass before swelling; m_1 is the sample mass when swelling equilibrium; m_2 is the sample mass after the final drying; φ is the mass fraction of the rubber in the composites; α is the mass loss fraction of the composites during swelling; ρ_r and ρ_s are the rubber and the solvent density, respectively, (0.9888 g/cm^3 for the rubber and 0.886 g/cm^3 for THF).

FTIR spectra for compound films were recorded by a Nexus 470 Fourier transform spectrometer. A thin film was produced by casting the blend in THF solution onto a Teflon slot die and drying it under conditions similar to those used in the bulk preparation. Spectra were obtained in a range of 4000–400 cm^{-1} by 32 scans at a resolution of 4 cm^{-1}.

High-resolution solid-state NMR spectra were obtained using a Bruker Avance-III 400 spectrometer operated at resonance frequencies of 100.62 MHz for carbon-13 under cross-polarization (CP) and magic angle sample spinning (MAS) conditions. An MAS rate of 5 kHz was used to eliminate resonance broadening attributed to the anisotropy of the chemical shift tensors. A cross polarization time of 2 ms was used for measuring the CP/MAS spectra. All the NMR experiments were conducted at room temperature.

DSC analyses were performed using a TA Q2000 instrument. Samples of approximately 4–6 mg in weight were sealed in hermetic aluminum pans and scanned at heating rates between 2.5 and 10 °C/min under a nitrogen flow of 50 mL/min. The calorimeter was calibrated with an empty aluminum pan as a reference.

KINETIC MODELS AND EQUATIONS

For the DSC method, it is common to assume that[23,24] the extent of reaction or the conversion, α is

proportional to the heat generated during the reaction, so the reaction rate can be expressed as

$$\frac{d\alpha}{dt} = k(T) \cdot f(\alpha) \tag{2}$$

where t is the time; $k(T)$ is the rate constant which is a temperature dependent function; $f(\alpha)$ is a conversion dependent function. An expression for $f(\alpha)$ has been used in this study: $(1 - \alpha)^n$. An integrated form of the above equation for $n \neq 1$ appears as

$$g(\alpha) = \int_0^\alpha \frac{d\alpha}{f(\alpha)} = \frac{(1-\alpha)^{1-n} - 1}{n-1} = k(T)t \tag{3}$$

where $g(\alpha)$ is the integrated form of a conversion dependent function. The dependence of the rate constant on temperature can be described by the Arrhenius expression

$$k(T) = A \cdot \exp\left(-\frac{E_a}{RT}\right) \tag{4}$$

where A is the frequency factor; E_a is the apparent activation energy; R is the universal gas constant.

For the kinetic analysis, the multiple-heating-rate models and the single-heating-rate model were employed. Three multiple-heating-rate methods that have been shown to be effective are Kissinger, Flynn–Wall–Ozawa, and Crane methods. A single overall reaction was assumed during curing considering the complexity of the reaction. Thus the obtained kinetic parameters represent all the processes that occur during curing.

The Kissinger model

According to the Kissinger method,[24–27] the activation energy can be obtained from the maximum reaction rate where $d^2\alpha/dt^2$ is zero under a constant-heating rate condition. The resulting relationship can be expressed as

$$\ln\left(\frac{\beta}{T_p^2}\right) = \ln\left(\frac{A \cdot R}{E_a}\right) - \frac{E_a}{R} \cdot \frac{1}{T_p} \tag{5}$$

Therefore, a plot of $\ln(\beta/T_p^2)$ versus $1/T_p$ gives E_a and A.

The Flynn–Wall–Ozawa model

The Flynn–Wall–Ozawa method yields a simple relationship between the apparent activation energy, the heating rate, and the isoconversion temperature,[14,23,28] giving the equation as

$$\log(\beta) = \log\left(\frac{A \cdot E_a}{R}\right) - 2.315 - 0.4567\frac{E_a}{RT_p} \tag{6}$$

Thus a plot of $\ln(\beta)$ versus $1/T_p$ gives both E_a and A.

The Crane model

Considering $d^2\alpha/dt^2 = 0$ at the peak exotherm,[24,26,27] and when $E_a/(nR) \gg 2T_p$, the Crane equation was obtained:

$$\frac{d(\ln\beta)}{d(1/T_p)} \approx -\frac{E_a}{nR} \tag{7}$$

Therefore, the n value could be obtained according to eq. (7).

The single-heating-rate model

The single-heating-rate model[25] is based on only a single constant heating rate cycle to determine parameters of the curing reaction. For nth-order reactions, a plot of $\ln[(d\alpha/dt)/(1 - \alpha)^n]$ against T^1 yields a linear relationship:

$$\ln\frac{d\alpha/dt}{(1-\alpha)^n} = \ln k(T) = \ln A - \frac{E_a}{RT} \tag{8}$$

The kinetic parameters $\ln A$ and E_a are thus determined from the intercept and slope.

RESULTS AND DISCUSSION

Crosslink density

In the equilibrium-swelling measurement, the crosslink density of the composites (ν_r) can be determined according to eq. (1), due to the balance[29] between the expansion force from swelling in the solvent and the contraction force produced by the rubber elasticity.

Figure 2 shows the effect of the curing time and the POSS content on the crosslink density (ν_r) of the composites. The result of the equilibrium-swelling experiment strongly suggested that HXNBR crosslinked with epoxycyclohexyl POSS under the investigated temperature. It can be seen that ν_r increased with the curing time until reaching balance or beginning to decrease. Meanwhile, ν_r increased greatly for samples with a higher content of epoxycyclohexyl POSS at the same curing time.

FTIR analysis

Figure 3 displays FTIR spectra of HXNBR, the compound, and the composite. According to Figure 3(a,b), the broad peaks at 3255 and 3535 cm^{-1} are assigned to the hydrogen bonding in HXNBR. The carboxyl C=O stretching absorption splits into two

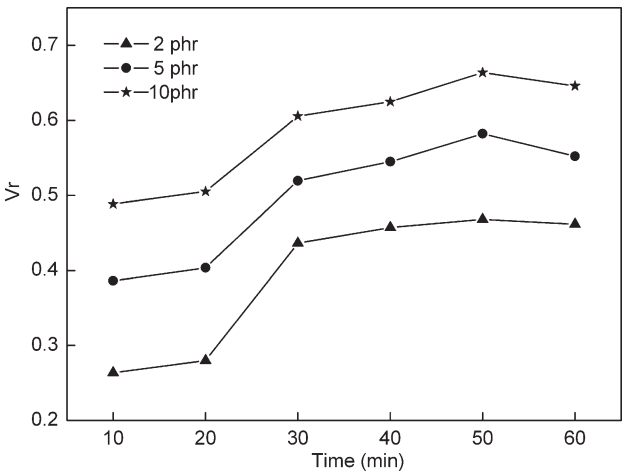

Figure 2 Curves of crosslink density versus curing time for composites with different POSS content: 2 phr, 5 phr, and 10 phr.

peaks. The peak at 1729 cm^{-1} is assigned to the free C= O stretch while that at 1697 cm^{-1} is assigned to the hydrogen bonded C=O stretch. The peak at 971 cm^{-1} is due to the C—O stretch of HXNBR while the 880 cm^{-1} peak is attributed to the epoxy group stretch of epoxycyclohexyl POSS. Besides, a strong Si—O—Si stretching peak was observed at about 1127 cm^{-1}, which is typical of silsesquioxane cages. For the composite, as shown in Figure 3(c), it is clear that the peaks at 880 and 971 cm^{-1} from the compound disappeared while new peaks at around 3384 and 1722 cm^{-1} were observed, which were respectively, assigned to the produced alcohol O—H and the ester C=O stretching vibrations of the composite. This implies that epoxycyclohexyl POSS reacted with HXNBR, forming the epoxycyclohexyl POSS/HXNBR composite. Assignments for the relevant

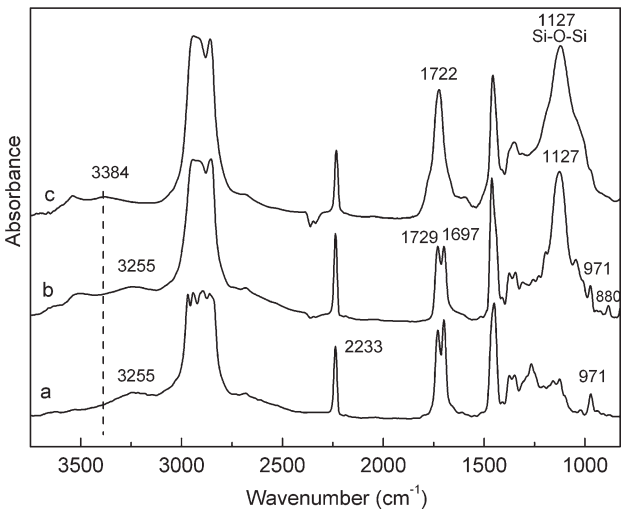

Figure 3 FTIR spectra: (a) HXNBR, (b) the 10 phr epoxycyclohexyl POSS/HXNBR compound, (c) the 10 phr epoxycyclohexyl POSS/HXNBR composite.

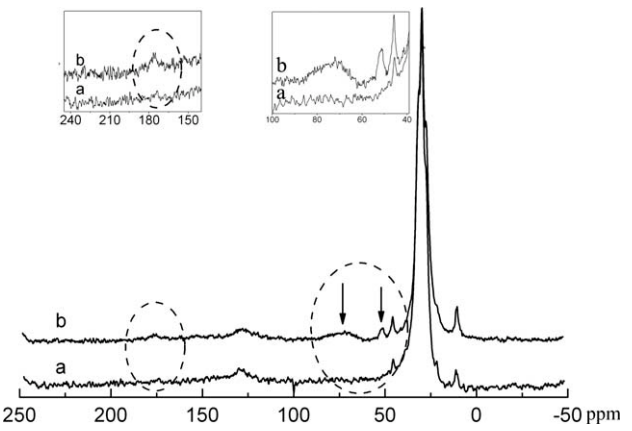

Figure 4 ^{13}C solid-state NMR spectra of HXNBR cured with epoxycyclohexyl POSS: (a) HXNBR, (b) the 10 phr epoxycyclohexyl POSS/HXNBR composite.

absorption bands[2,8,30,31] have been given in several publications.

Solid-state ^{13}C-NMR analysis

Figure 4 shows the ^{13}C solid-state NMR spectra of HXNBR and the composite. The basic spectrum features of the two samples are similar except the new ones clearly evidenced in Figure 4(b): the broad line in the region 68–77 ppm and the line at 51.4 ppm are attributed to the C—O groups (C—OH or C—OR) of the epoxycyclohexyl POSS/HXNBR composite, according to earlier reports[32–36] in the literature.

Based on the FTIR and the ^{13}C solid-state NMR analyses, together with earlier reports[28] about the curing reactions involving ester and ether formation, the possible reaction in the curing process of HXNBR with epoxycyclohexyl POSS is displayed in Scheme 1(a,b).

Curing kinetic analysis

Figure 5 shows DSC thermograms of the 40 phr epoxycyclohexyl POSS/HXNBR compound at the conducting rates between 2.5 and 10 °C/min. As the heating rate was increasing, the exothermic temperature was shifted to a high temperature, which is in accordance with the early report of Chen et al.[37] Table I summarizes the results of the temperature at the peak of the thermograms (T_p) and the conversion at the peak (α_p) of the DSC thermograms for all the compounds, which shows that T_p and α_p of the reaction were influenced by the content of POSS.

Determination of kinetic parameters with Kissinger and Flynn–Wall–Ozawa methods

Applying Kissinger and Flynn–Wall–Ozawa methods to the maximum reaction rate, linear

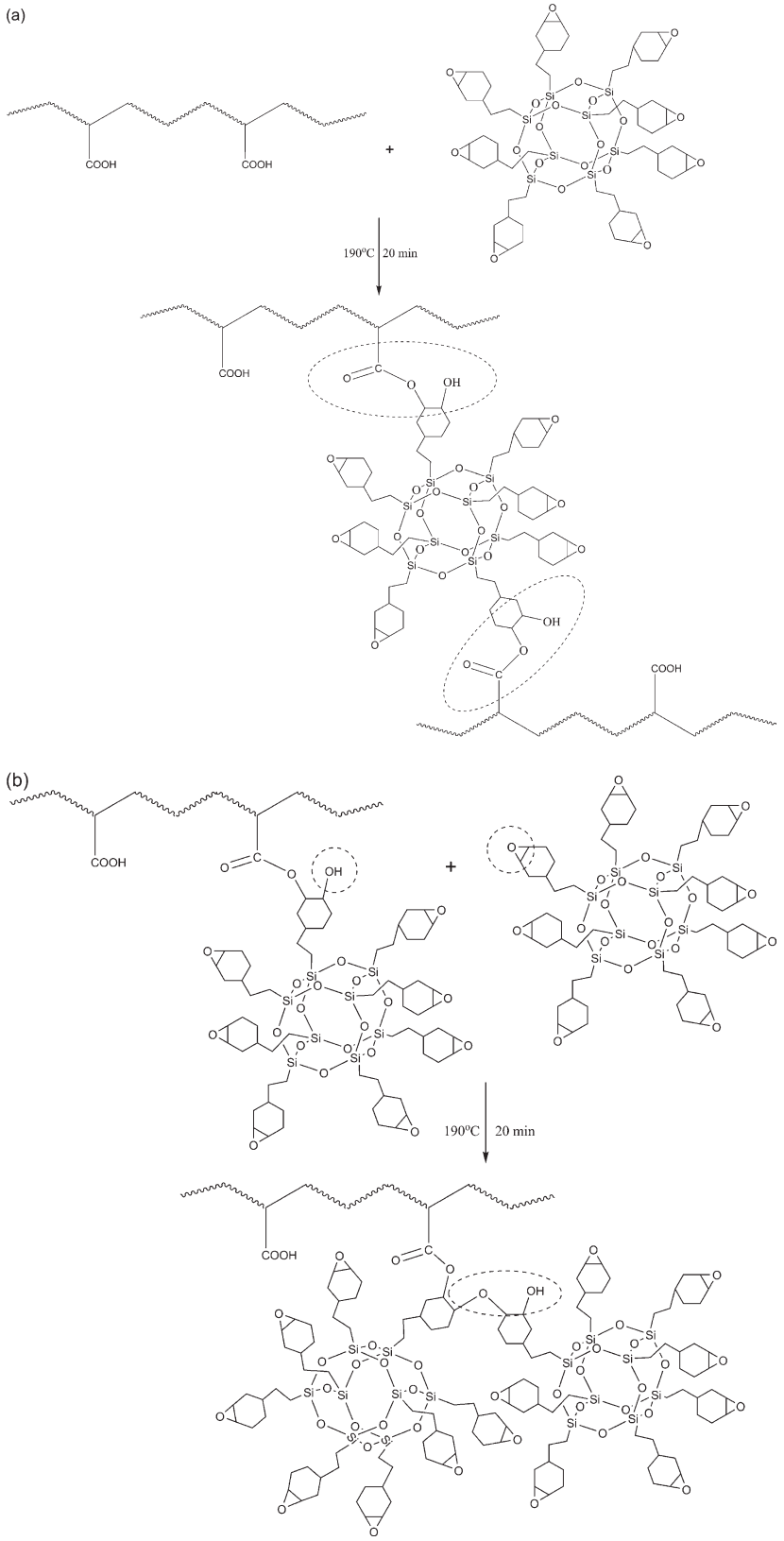

Scheme 1 Possible reactions of epoxycyclohexyl POSS/HXNBR: (a) and (b).

relationships were obtained by plotting $\ln\beta/T_p^2$ against $1/T_p$, and $\ln\beta$ against $1/T_p$, confirming the validity of the models. The plots for the compound with 2 phr POSS were given in Figure 6. Table II summarizes the obtained kinetic parameters and coefficients of correlation (R-square) for compounds

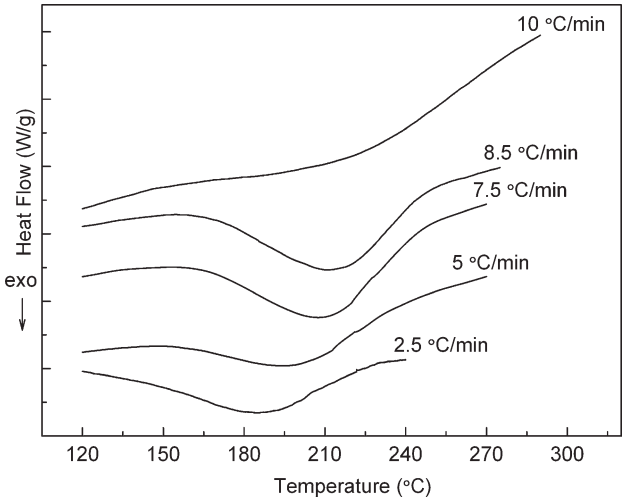

Figure 5 Dynamic DSC thermograms at different heating rates for the compound with 40 phr epoxycyclohexyl POSS.

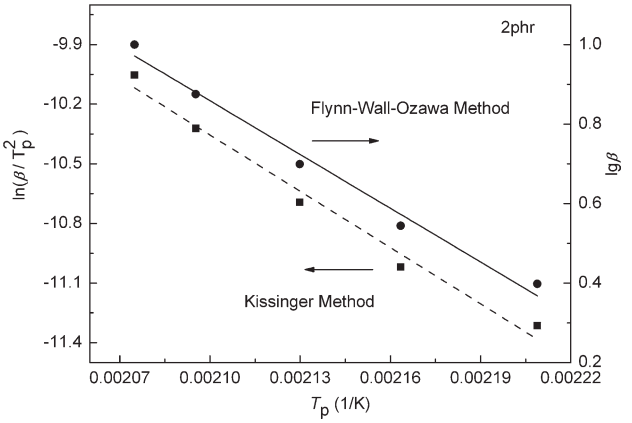

Figure 6 Plots for determination of E_a and A with Kissinger and Flynn–Wall–Ozawa methods for compound with 2 phr POSS.

with different POSS contents. As shown in Table II, the values of E_a are respectively, 57.46–78.50 and 62.07–82.04 kJ/mol by using Kissinger and Flynn–Wall–Ozawa methods, which are in agreement with the values of early literature.[2] Correspondingly, for the napierian logarithm of the frequency factor (ln$A$), the values are 12.86–18.63 and 14.73–19.90, respectively. The parameters obtained with the Flynn–Wall–Ozawa model are slightly higher than those obtained with the Kissinger model because the two models are based on different specific assumptions. The POSS content has effect on E_a, implying that[14,23] compounds with different POSS contents have different reactivities, which is because the presence of an increased number of multifunctional monomers contributes to increased differences in the reactivity of POSS.

TABLE I
Peak Temperature, T_p, and Conversion at the Peak Exotherm, α_p, at Different Heating Rates, β

POSS content	β (°C/min)	T_p (°C)	α_p
2 phr	2.5	179.6	0.57
	3.5	189.1	0.59
	5	196.4	0.64
	7.5	204.1	0.64
	10	208.8	0.65
5 phr	2.5	178.8	0.56
	5	195.0	0.55
	6	200.7	0.58
	7.5	210.9	0.63
	10	215.2	0.60
10 phr	2.5	177.1	0.53
	5	190.8	0.49
	7	198.6	0.51
	8.5	203.2	0.61
	10	206.3	0.50
40 phr	2.5	184.8	0.49
	5	197.8	0.51
	7.5	209.7	0.57
	8.5	212.8	0.56
	10	219.2	0.61

Determination of the overall reaction order (n) with the Crane method

The overall reaction order (n) during curing can be obtained by the Crane method, according to eq. (7). Linear relationships were obtained by plotting lnβ versus $1/T_p$, confirming the validity of the model. The plot for the compound with 2 phr POSS was given in Figure 7. The calculated reaction order (n) based on the value of the slope ($-E_a/nR$) and the coefficients of correlation were given in Table III for compounds with different POSS contents. As displayed in Table III, The reaction order (n) obtained with the Kissinger method and Flynn–Wall–Ozawa method were 0.88–0.93 and 0.95–0.97 respectively, both of which were close to 1.

Determination of kinetic parameters with the isoconversion Flynn–Wall–Ozawa method

The plot of lnβ versus $1/T_i$ (T_i, isoconversion temperature) enables the calculation of E_a at any conversion (α) with the isoconversion Flynn–Wall–Ozawa method, according to eq. (6). Plots of the conversion (α) versus the dynamic temperature (T) for the 2 phr POSS/HXNBR compound are given in Figure 8. Plots of lnβ versus $1/T_i$ for the 2 phr POSS/HXNBR compound are shown in Figure 9, with the conversion from 10 to 90%. The obtained kinetic parameters and coefficients of correlation were given in Table IV. In the same way, the average values of parameters with the respective standard deviations (SD) for compounds with different POSS contents are also given in Table IV. It can be seen from the Table IV that the model fit well with the

TABLE II
Kinetic Parameters and Coefficients of Correlation Evaluated with Kissinger and Flynn–Wall–Ozawa Methods

	Kissinger			Flynn-Wall-Ozawa		
POSS (phr)	E_a (kJ/mol)	ln$A$	R-square	E_a (kJ/mol)	ln$A$	R-square
2	78.50	18.63	0.9787	82.04	19.90	0.9820
5	57.46	12.86	0.9769	62.07	14.73	0.9822
10	76.64	18.31	0.9989	80.22	19.61	0.9991
40	67.83	15.54	0.9789	72.00	17.12	0.9833

experimental data. The average E_a for the compound with the different POSS contents is 70.34–92.35 kJ/mol, showing its dependence on the POSS content. This is because the presence of an increased number of multifunctional monomers contributes to increased differences in the reactivity of the POSS.

Analysis of the dynamic DSC data by the single-heating-rate model

Kinetic parameters at the each heating rate were obtained by plotting ln$k$ versus $1/T$ according to the single-heating-rate model, considering a single overall curing process. Figure 10 shows plots of ln$k$ versus $1/T$ for the 2 phr POSS/HXNBR compound. The obtained kinetic parameters and coefficients of correlation were given in Table V. Similarly, the average values of parameters with the respective standard deviations (SD) are also given in Table V. It is found that the average R-square for the compound with the different POSS contents is 0.9919–0.9949, consist-

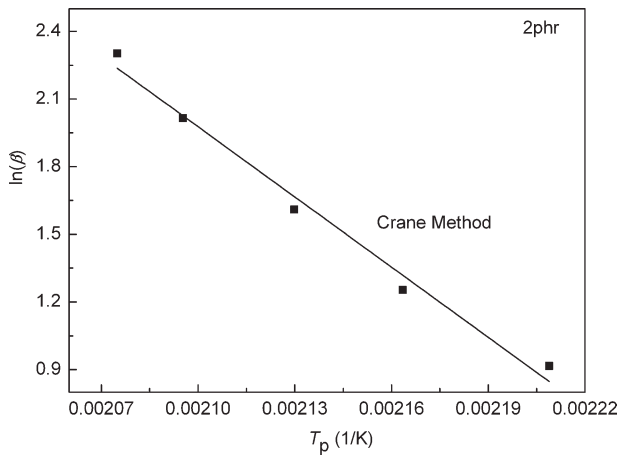

Figure 7 Plot of lnβ versus $1/T_p$ with the Crane method for compound with 2 phr POSS.

TABLE III
Values of the Overall Reaction Order, n, and Coefficients of Correlation, Obtained with the Crane Method

POSS (phr)	E_a/nR	R-square	n^a	n^b
2	10376.1	0.9820	0.93	0.97
5	7850.4	0.9822	0.88	0.95
10	10146.6	0.9991	0.91	0.95
40	9106.9	0.9833	0.90	0.95

[a] Using the value of E_a obtained with the Kissinger method.
[b] Using the value of E_a obtained with the Flynn–Wall–Ozawa method.

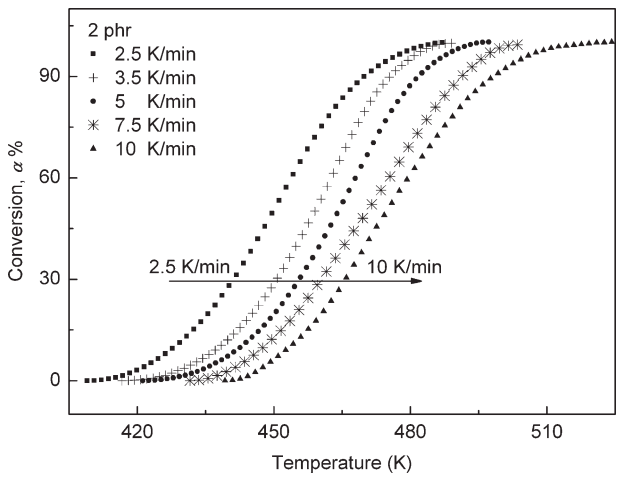

Figure 8 Plots of conversion versus temperature for DSC curves of the 2 phr POSS/HXNBR compound.

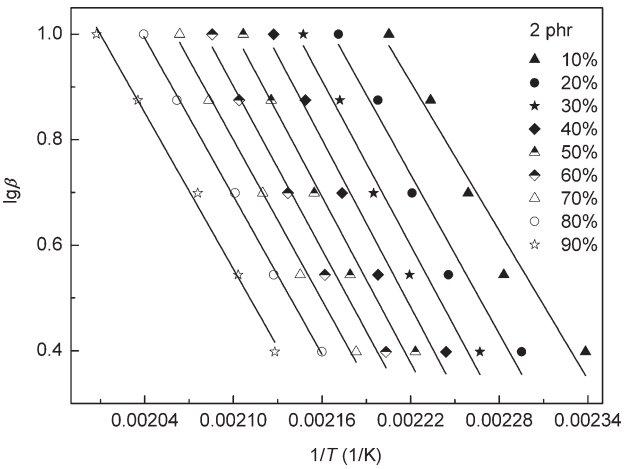

Figure 9 Plots of lnβ versus $1/T$ under different conversions for the 2 phr POSS/HXNBR compound.

TABLE IV
Kinetic Parameters with the Iso-Conversional Flynn–Wall–Ozawa Method

POSS content	Conversion, α %	E_a (kJ/mol)	ln$A$	R-square
2 phr	10	85.53	19.95	0.9499
	20	91.74	21.97	0.9568
	30	94.85	22.96	0.9576
	40	96.40	23.47	0.9630
	50	95.53	23.30	0.9721
	60	94.00	22.94	0.9825
	70	92.26	22.53	0.9921
	80	90.89	22.22	0.9978
	90	89.89	22.00	0.9936

POSS content	Average E_a (kJ/mol)	SD[a]	Average ln$A$	SD[a]	Average R-square	SD[a]
2 phr	92.35	3.36	22.37	1.06	0.9739	0.0181
5 phr	70.34	8.87	16.50	2.42	0.9904	0.0099
10 phr	77.13	3.15	18.35	0.53	0.9950	0.0036
40 phr	89.38	4.96	21.14	1.35	0.9909	0.0026

[a] Standard deviation.

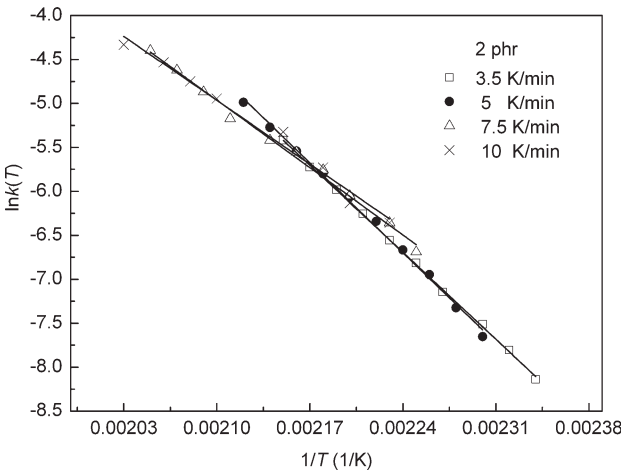

Figure 10 Plots of ln$k$ versus $1/T$ by the single-heating-rate model for the 2 phr POSS/HXNBR compound.

ent to the research by Gao et al.,[38] which is close to 1, indicating that the model fit well with the experimental data. According to Figure 10, for a given temperature, the rate constant (k) did not show much dependence on the heating rate (β). The obtained E_a showed dependence on the heating rate and the POSS content, and the average E_a for the compound with a fixed POSS content, 66.90–104.13 kJ/mol, was greater than that obtained with Kissinger and Flynn–Wall–Ozawa methods which were applied to the maximum reaction rate.

According to eq. (8), the curves of the calculated reaction rate ($d\alpha/dt$) versus temperature, based on E_a and A at each heating rate by the single-heating-rate model, were compared with the experimental data. Figure 11 showed the curves for the 2 phr POSS/HXNBR compound at the heating rate of 10 K/min. It can be seen that the calculated curve fit well with the experimental data in spite of a slight

TABLE V
Kinetic Parameters Obtained by the Single-Heating-Rate Model

POSS content	β (°C/min)	E_a (kJ/mol)	ln$A$	R-square
2 phr	3.5	117.62	25.00	0.9994
	5	121.59	26.06	0.9966
	7.5	91.06	18.04	0.9931
	10	86.25	16.82	0.9826

POSS content	Average E_a (kJ/mol)	SD[a]	Average ln$A$	SD[a]	Average R-square	SD[a]
2 phr	104.13	18.05	21.48	4.72	0.9929	0.0073
5 phr	66.90	5.39	11.36	1.37	0.9949	0.0025
10 phr	85.12	7.37	16.35	1.87	0.9919	0.0055
40 phr	89.17	7.34	17.00	1.87	0.9941	0.0032

[a] Standard deviation.

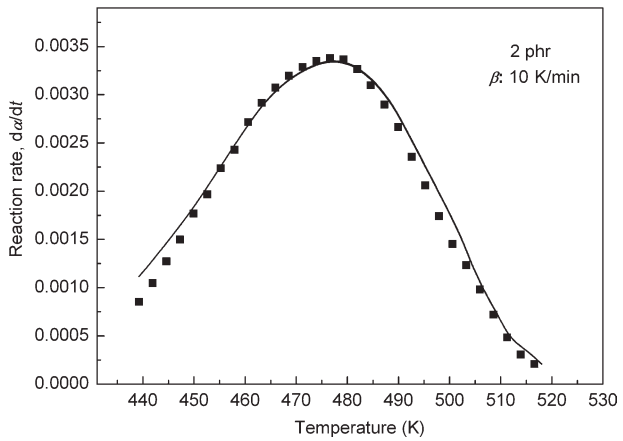

Figure 11 The calculated reaction rate $d\alpha/dt$ versus temperature curve (–) and the experimental reaction rate $d\alpha/dt$ versus temperature curve (■■■) at the heating rate of 10 K/min for the 2 phr POSS/HXNBR compound.

discrepancy, which may result from that a single overall curing process has been considered in the kinetic analysis while two reactions may have occurred during curing,[14] as displayed in Scheme 1. Another reason may be that errors will inevitably be introduced in the data processing.

CONCLUSIONS

A new organic–inorganic hybrid material was prepared through reactive blending of HXNBR and epoxycyclohexyl POSS, and its curing kinetics was investigated using the DSC method by the multiple-heating-rate models (the Kissinger, Flynn–Wall–Ozawa, and Crane methods) as well as the single-heating-rate model.

From the kinetic analysis, it can be concluded that the models employed fit well with the curing system under study. The apparent activation energy (E_a) and Arrhenius frequency factor (A) obtained by the multiple-heating-rate models showed dependence on the POSS content and the heating rate β. The obtained overall reaction order n was practically constant and close to 1. The isoconversion Flynn–Wall–Ozawa method was also performed and fit well in the study.

By the single-heating-rate model, E_a and A also showed dependence on the heating rate (β). However, the rate constant (k) did not show much dependence on it. The average E_a for the compound with a certain POSS content, 66.90–104.13 kJ/mol, was greater than that obtained with Kissinger and the Flynn–Wall–Ozawa methods.

References

1. Huang, J.; He, C.; Liu, X.; Xu, J.; Tayand, C. S. S.; Chow, S. Y. Polymer 2005, 46, 7018.
2. Herman Teo, J. K.; Teo, K. C.; Pan, B.; Xiaoand, Y.; Lu, X. Polymer 2007, 48, 5671.
3. Abad, M. J.; Barral, L.; Fasceand, D. P.; Williams, R. J. J. Macromolecules 2003, 36, 3128.
4. Matejka, L.; Strachota, A.; Plestil, J.; Whelan, P.; Steinhartand, M.; Slouf, M. Macromolecules 2004, 37, 9449.
5. Strachota, A.; Kroutilova, I.; Kovarovaand, J.; Matejka, L. Macromolecules 2004, 37, 9457.
6. Bian, Y.; Pejanovic, S.; Kennyand, J.; Mijovic, J. Macromolecules 2007, 40, 6239.
7. Yei, D.-R.; Kuo, S.-W.; Suand, Y.-C.; Chang, F.-C. Polymer 2004, 45, 2633.
8. Xu, H.; Kuo, S.-W.; Leeand, J.-S.; Chang, F.-C. Macromolecules 2002, 35, 8788.
9. Xu, H.; Yang, B.; Wang, J.; Guangand, S.; Li, C. Macromolecules 2005, 38, 10455.
10. Seurerand, B.; Coughlin, E. B. Macromol Chem Phys 2008, 209, 1198.
11. Fina, A.; Tabuani, D.; Peijsand, T.; Camino, G. Polymer 2009, 50, 218.
12. Choi, J.; Kimand, S. G.; Laine, R. M. Macromolecules 2003, 37, 99.
13. Xiao, F.; Sun, Y.; Xiuand, Y.; Wong, C. P. J Appl Polym Sci 2007, 104, 2113.
14. Martín, J. L. Polymer 1999, 40, 3451.
15. Girard-Reydet, E.; Riccardi, C. C.; Sautereauand, H.; Pascault, J. P. Macromolecules 2002, 28, 7608.
16. Lu, L.; Zhai, Y.; Zhang, Y.; Ongand, C.; Guo, S. Appl Surf Sci 2008, 255, 2162.
17. Sun, G.; Sun, H.; Liu, Y.; Zhao, B.; Zhuand, N.; Hu, K. Polymer 2007, 48, 330.
18. Li, S.; Vatanparastand, R.; Lemmetyinen, H. Polymer 2000, 41, 5571.
19. Domínguez, J. C.; Alonso, M. V.; Olietand, M.; Rodríguez, F. Eur Polym J 2010, 46, 50.
20. Li, G.; Huang, Z.; Li, P.; Xin, C.; Jia, X.; Wang, B.; He, Y.; Ryuand, S.; Yang, X. Thermochim Acta 2010, 497, 27.
21. Rocks, J.; Rintoul, L.; Vohwinkeland, F.; George, G. Polymer 2004, 45, 6799.
22. Guo, B.; Lei, Y.; Chen, F.; Liu, X.; Duand, M.; Jia, D. Appl Surf Sci 2008, 255, 2715.
23. Barral, L.; Cano, J.; López, J.; López-Bueno, I.; Nogueira, P.; Abadand, M. J.; Ramírez, C. Polymer 2000, 41, 2657.
24. Yan, H.-q.; Chenand, S.; Qi, G.-r. Polymer 2003, 44, 7861.
25. Boeyand, F. Y. C.; Qiang, W. Polymer 2000, 41, 2081.
26. Xu, K.; Chen, M.; Zhangand, K.; Hu, J. Polymer 2004, 45, 1133.
27. Liu, W.; Qiu, Q.; Wang, J.; Huoand, Z.; Sun, H. Polymer 2008, 49, 4399.
28. Pielichowski, K.; Czuband, P.; Pielichowski, J. Polymer 2000, 41, 4381.
29. Moriand, M.; Koenig, J. L. J Appl Polym Sci 1998, 70, 1391.
30. Senichand, G. A.; MacKnight, W. J. Macromolecules 2002, 13, 106.
31. Liu, H.; Zhengand, S.; Nie, K. Macromolecules 2005, 38, 5088.
32. Cheung, M. K.; Wang, J.; Zhengand, S.; Mi, Y. Polymer 2000, 41, 1469.
33. Wang, J.; Cheungand, M. K.; Mi, Y. Polymer 2002, 43, 1357.
34. Zhang, X.; Goldingand, J.; Burgar, I. Polymer 2002, 43, 5791.
35. Zhang, X.; Burgar, I.; Lourbakosand, E.; Beh, H. Polymer 2004, 45, 3305.
36. Palmas, P.; Colsenet, R.; Lemariéand, L.; Sebban, M. Polymer 2003, 44, 4889.
37. Chen, W.-Y.; Wang, Y.-Z.; Kuo, S.-W.; Huang, C.-F.; Tungand, P.-H.; Chang, F.-C. Polymer 2004, 45, 6897.
38. Gao, J.; Jiangand, C.; Zhang, X. Int J Polym Mater 2007, 56, 65.